Proceedings of the 2003 IEEE/RSJ
Intl. Conference on Intelligent Robots and Systems
Las Vegas, Nevada · October 2003

A Study on the Environmental Map Building for a Mobile Robot Using Infrared Range-finder Sensors

Heon-Hui Kim
Department of Control and Instrumentation Engineering
Korea Maritime University
Yeongdo-Gu, Busan, Korea
kimhh@bada.hhu.ac.kr

Yun-Su Ha
Division of Mechanical and Information Engineering
Korea Maritime University
Yeongdo-Gu, Busan, Korea
hys@hanara.kmaritime.ac.kr

Gang-Gyoo Jin
Division of Mechanical and Information Engineering
Korea Maritime University
Yeongdo-Gu, Busan, Korea
ggjin@hanara.kmaritime.ac.kr

Abstract – This paper presents a methodology for building the high accuracy environmental map using a mobile robot. The design approach uses low cost infrared range-finder sensors incorporating with neural networks. To enhance the map quality, the errors occurring from the sensors are corrected. The nonlinearity error of the sensors is compensated using a backpropagation neural network and the random error of readings including the uncertainty of environment is taken into a sensor model at probabilistic approach. The map is represented by occupancy grid framework and updated by the Bayesian estimation mechanism. The effectiveness of the proposed method is verified through a series of experiments (see video).

I. INTRODUCTION

Building a high accuracy environmental map continues to be one of the most demanding problems in the field of mobile robot. Most mobile robots have employed visual sensors, such as ultrasonic sensor, laser range-finder and CCD camera to build their environmental maps. The use of laser range-finder and CCD camera insures relatively high quality information, but it requires high sensing cost.

A number of works for applying ultrasonic sensors to map building have been reported. A method proposed by Elfes[1] is based on the probabilistic model for readings of ultrasonic sensors, which has the occupancy grid framework. Moravec and Cho[2] presented an approach where sensor fault is taken into consideration in probabilistic sensor model. However, shortcomings of their methods are that there are able to be limitations to enhance the map quality due to physical restrictions, such as large beam opening angle, specular reflection of ultrasonic sensors and so on[3].

Recently more attention has been given to the use of low-cost sensors like infrared range-finder sensors in map building for mobile robots. Although infrared range-finder sensors provide less quality than other visual sensors, they have the advantage of low sensing cost and provide distant and directional information about an object. To achieve successful goals with such sensors, their characteristics should be analyzed.

This paper presents a methodology for building an environmental map using a mobile robot with infrared range-finder sensors. An approach is therefore developed to correct the nonlinearity error of infrared range finder sensors and the random error of readings based on neural networks and a probabilistic approach. In this approach, the map is represented by occupancy grid framework and updated by the Bayesian estimation mechanism. The effectiveness of the proposed method is verified through a series of experiments.

II. INFRARED RANGE FINDER

A. Structure and Specifications

The sensor adopted for this work is infrared range-finder PB9-01 manufactured by HOKUYO AUTOMATIC CO., LTD, which uses an infrared LED modulated at 870nm for signal generation. It not only has compact size and light weight but also gets distant and directional information to an object for one time scanning. Fig. 1 and Fig.2 show the structure and scan process of PB9-01.

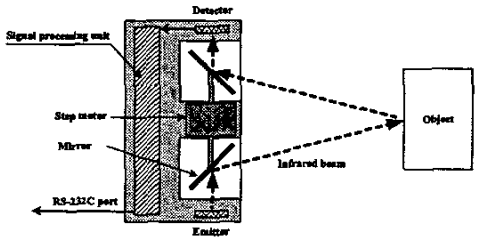

Fig. 1 Structure of PB9-01

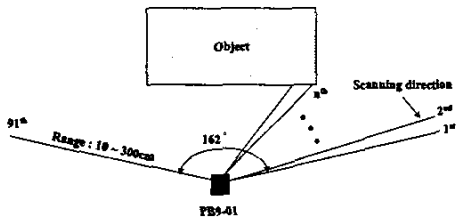

Fig. 2 Scan process of PB9-01

Although it is not recommendable for the use at outdoor environment due to its short detecting range and the interference by sunlight, PB9-01 is applicable to the environmental recognition system of a small indoor mobile robot. Table I illustrates its specifications.

TABLE I
Specifications of PB9-01

Items	Specifications
Size	70×60×120mm
Total weight	500g
Resolution of directional angle	1.78°
Scanning range	162°
Range of distance	10~300cm
Interface method	RS232C
Response time	160ms or less
Power source	DC24V

B. Analysis of Sensor Characteristics

The quality of map is highly related to sensor characteristics, that is, accuracy, precision and linearity. In order to enhance the accuracy of environmental map, It is necessary to analyze the characteristics of the sensor based on data obtained through experiments. Hence, a series of tests were performed by measuring the distance while changing the location of a plate in front of a mobile robot with PB9-01 in range of 10 to 300cm. For every space of 10cm, distance data of 200 were collected and they were averaged. Fig. 3(a) shows that there exist both the error between actual distance and measured distance due to mainly nonlinearity and the random error in readings. It can be seen in Fig. 3(b) that the distribution of sample data is approximately Gaussian. Standard deviation is approximated as a second-order polynomial as depicted in Fig. 3(c). By applying the least squares method, the polynomial is of the following form:

$$\sigma(d) = 0.0001d^2 - 0.0017d + 0.7544 \quad (1)$$

where, d is the measured distance.

In general, the random error of reading can be readily corrected by one of probabilistic approaches but the nonlinearity error can not be done in such a way. Hence, correction of this type of error is taken into consideration in the next section.

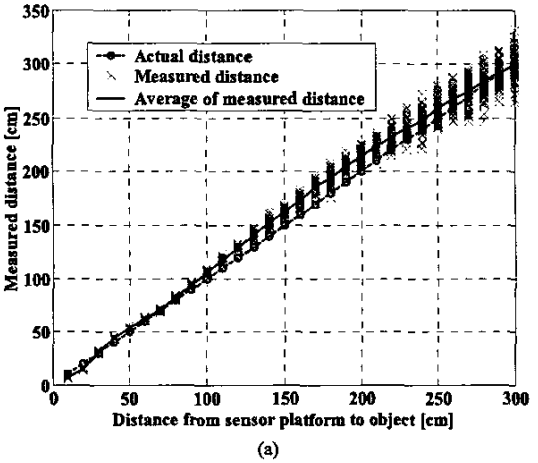

(a)

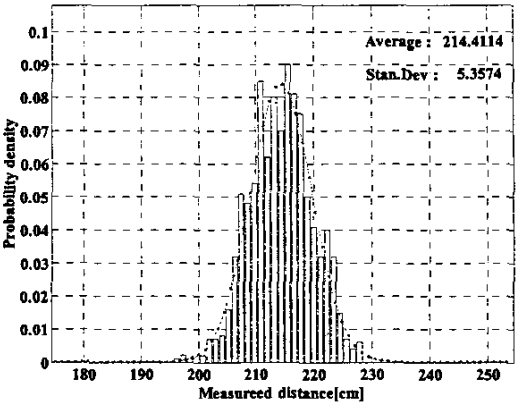

(b)

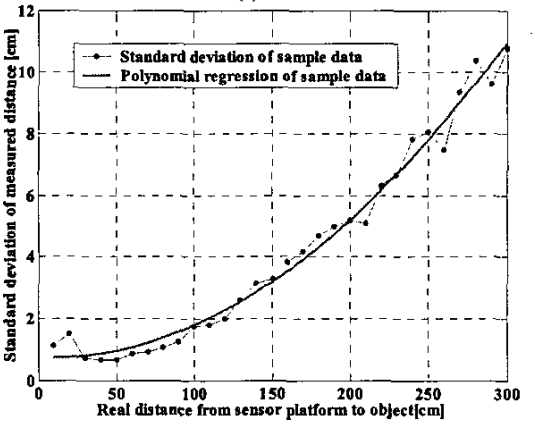

(c)

Fig. 3 Characteristics of Pb9-01
(a) Distance measurement, (b) Probability distribution of measured data at 200cm (c) Standard deviation

III. SENSOR BASED MAP BUILDING

In this paper, the environmental map for the mobile robot is represented as an occupancy grid framework. The occupancy grid is a two-dimensional tessellation of space into cells, where each cell stores a probabilistic estimated value of its state. In map building, we regarded the robot position obtained from the odometry as the absolute position. And we ignored the error due to the resolution of the scanning angle of PB9-01 because the resolution is 1.78 degree, enough for map building. Hence, sensor data on each step in scan range can be represented as 1-dimemsional array of the distance reading to the object.

The process of environmental map building is shown in Fig. 4. Sensor readings are corrected by a neural network-based algorithm and then converted to the occupancy information of each cell with a probabilistic value. The map is built by integrating the probabilistic information of each cell, and updated based on Bayesian inference.

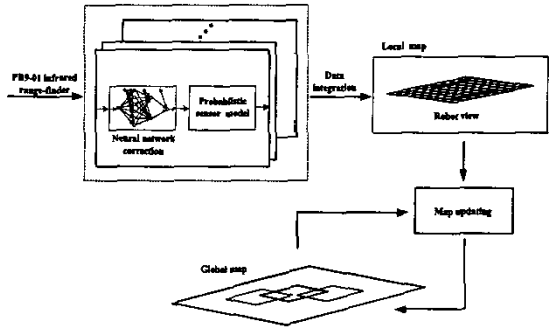

Fig. 4 Environmental map building process using PB9-01

A. Correction of Nonlinearity using Neural Networks

The quality of map depends upon the characteristics of the sensor, mainly the accuracy of the sensing position and the performance of a fusion algorithm. To cope with the error occurring from the nonlinearity of PB9-01, a neural network(NN) is incorporated. The NN has architecture of a four-layered network. The single-input single-output NN has six nodes and two nodes in the first and second hidden layers, respectively. The hyperbolic tangent and linear transfer functions are used to the hidden layers and the output layer, respectively.

Once the structure of the NN is determined, the next procedure is training. Fig. 5 shows the training configuration. The training procedure involves the presentation of a set of pairs of input and output patterns and a training rule. The input pattern is the average of readings from the sensor platform to the object and the target or output pattern is its actual distance. The NN uses the input to produce its own output and then compare it with the target pattern.

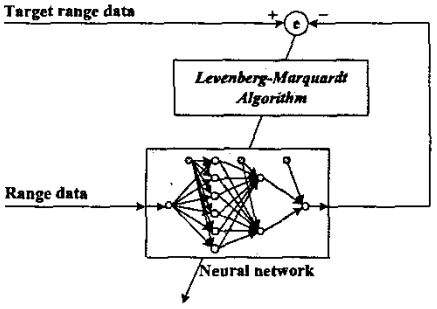

Fig. 5 Training mechanism of the NN

If there is difference between the network output and the target pattern, then interconnection weights between the nodes are changed to reduce the difference by a training rule. The Levenberg-Marquardt algorithm which is an extension of the backpropagation algorithm is adopted for this network. The learning rate is set to 0.01 and training is terminated less than rms error of 2.5×10^{-5}. Finally, weight and bias vectors for the neural network were determined as (2).

$$W_1 = \begin{bmatrix} -5.7950 \\ -6.2927 \\ -2.9562 \\ 2.4116 \\ -4.3381 \\ -5.4769 \end{bmatrix}, \quad b_1 = \begin{bmatrix} 18.3913 \\ 16.7640 \\ 6.5854 \\ -2.8336 \\ 2.4960 \\ -1.0804 \end{bmatrix}$$

$$W_2^T = \begin{bmatrix} 0.1691 & 1.8179 \\ 3.5284 & 0.6239 \\ 0.4716 & -0.3999 \\ -0.1736 & -2.5846 \\ 0.0987 & -0.1048 \\ 0.6648 & -1.6205 \end{bmatrix}, \quad b_2 = \begin{bmatrix} -3.9994 \\ -0.7220 \end{bmatrix} \qquad (2)$$

$$W_3 = \begin{bmatrix} -2.6751 & -0.4954 \end{bmatrix}, \quad b_3 = 0.1639$$

Performances of the trained NN corrector are depicted in Fig. 6 and Fig. 7. Fig. 6 shows the result of experiment performed under the same condition as Fig. 3(a). As the result, the non-linear bias is remarkably decreased as compared with Fig. 3(a).

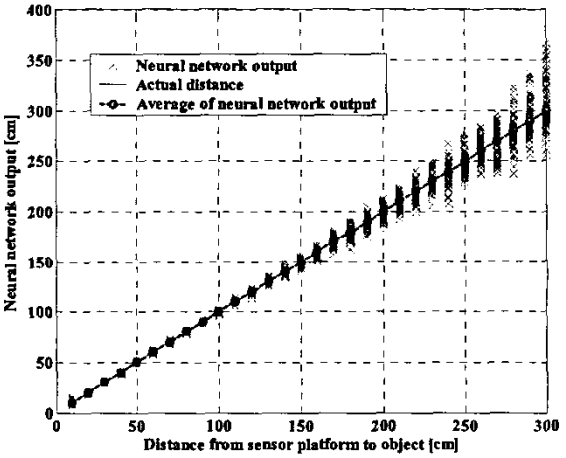

Fig. 6 Result of correction using the NN(case 1)

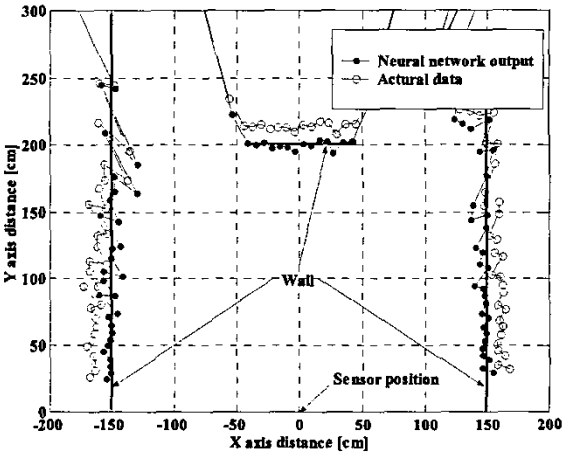

Fig. 7 Result corrected using the NN(case 2)

Fig. 7 shows that of experiment performed under different an environment. In this case, also corrected data provide good approximate to real world better than direct sensor readings.

B. Map Updating Formula

The probability variable $p(o_x)$ associated with a cell x is represented by the probability that the cell x is occupied, and $\overline{o}$ represents the alternative to the event o. For two occupancy possibilities o and $\overline{o}$ of a cell, new information z_1 and *a priori* information z_2, one form of Bayes' theorem[4] gives:

$$p(o \mid z_2 \wedge z_1) = \frac{p(z_2 \mid o \wedge z_1)p(o \mid z_1)}{p(z_2 \mid o \wedge z_1)p(o \mid z_1) + p(z_2 \mid \overline{o} \wedge z_1)p(\overline{o} \mid z_1)} \tag{3}$$

Dividing (3) by $p(\overline{o} \mid z_2 \wedge z_1)$ described in a similar manner and rearranging, (4) is obtained as:

$$\frac{p(o \mid z_2 \wedge z_1)}{p(\overline{o} \mid z_2 \wedge z_1)} = \frac{p(z_2 \mid o \wedge z_1)p(o \mid z_1)}{p(z_2 \mid \overline{o} \wedge z_1)p(\overline{o} \mid z_1)} \tag{4}$$

Also, applying to only information z, instead of z_1 and z_2 in (4) yields

$$\frac{p(o \mid z)}{p(\overline{o} \mid z)} = \frac{p(z \mid o)p(o)}{p(z \mid \overline{o})p(\overline{o})} \tag{5}$$

In the case of z_1 and z_2 are statistically independent, $p(o \mid z_1 \wedge z_2)$ is given by $p(o \mid z_1) \wedge p(o \mid z_2)$, thus allowing z_1 and z_2 to be incorporated into the map. This is not possible in general because the two measurements may interact in some way. For instance, either z_1 or z_2 along may indicate a high probability of o, but taken together, they may confirm some other hypothesis, and reduce the probability of o. We assume that the sensor errors are independent from one reading z_2 to a priori information z_1 for map combining, in this paper. That is,

$$\frac{p(z_2 \mid o \wedge z_1)}{p(z_2 \mid \overline{o} \wedge z_1)} = \frac{p(z_2 \mid o)}{p(z_2 \mid \overline{o})} \tag{6}$$

Therefore, the following equation is obtained by (4), (5) and (6).

$$\frac{p(o \mid z_1 \wedge z_2)}{p(\overline{o} \mid z_1 \wedge z_2)} = \frac{p(o \mid z_1)p(o \mid z_2)p(\overline{o})}{p(\overline{o} \mid z_1)p(\overline{o} \mid z_2)p(o)} \tag{7}$$

It is assumed that a priori probability $p(o)$ of cell occupation is the average of space density. When the information z_2 is a sensor reading, $p(z_2 \mid o)/p(z_2 \mid \overline{o})$, for all cells and all possible readings, is called the sensor model[5].

C. Probabilistic Sensor Model

The occupancy probability about a cell is approximated to Gaussian distribution such as

$$\mathrm{p}(z,r) = \frac{1}{\sqrt{2\pi\sigma}} \exp\left[\frac{-(r-z)^2}{2\sigma^2}\right] \tag{8}$$

where z is measured distance, r is the distance from sensor location to the center point of corresponding cell and σ is standard deviation as (1).

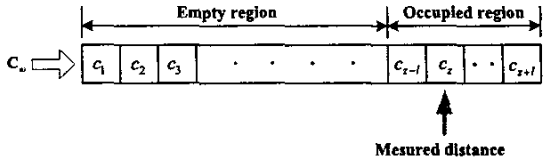

Fig. 8 One-dimensional array for sensor model

These cells are divided into two regions. One is "empty region" satisfying $r < z - 2\sigma$ and the other is "occupied region" satisfying $z - 2\sigma \le r \le z + 2\sigma$. Each cell c_i in the real world is assumed to be either empty or occupied. In the use of PB9-01, it can not be expected always for successful sensing, because the specular reflection of infrared light may exist. Hence, a fault sensing is considered in sensor modeling.

Let's p_i^{det} be the probability that the sensing beam will be stopped at a particular cell if it should happen to be occupied, and p_i^{fal} be the probability that the beam will be stopped at an empty cell. These probability functions are defined by measurement distance as

$$p^{det} = 1 - \left(r / R_{\max}\right)^2 \tag{9}$$

$$p^{fal} = \alpha \cdot p^{det} \tag{10}$$

where $R_{\max}$ is maximum detection range of the sensor and α is a weight factor. At any time, the robot has only an occupancy estimate $p(o_i)$ for each cell, derive from prior information. A reading updates this estimate. In this circumstance, the probability that a wave front will be stopped at c_i can be estimated by combining the two possibilities, weighted by their probability.

$$\mathrm{P}(p_i^{halt}) = p(o_i) \cdot p_i^{det} + p(\overline{o}_i) \cdot p_i^{fal} \tag{11}$$

We model the sensor as emitting a signal, which hits each of the cells in its path in the order of their distance from the sensor, until it detects an occupied cell[6]. It is represented by

$$\frac{p(z \mid o)}{p(z \mid \overline{o})} = \frac{\sum_{k=1}^{n} p_k^z \mathrm{P}(p_k^{halt} \mid o_j) \prod_{i=1}^{k-1} \overline{\mathrm{P}(p_i^{halt} \mid o_j)}}{\sum_{k=1}^{n} p_k^z \mathrm{P}(p_k^{halt} \mid \overline{o}_j) \prod_{i=1}^{k-1} \overline{\mathrm{P}(p_i^{halt} \mid \overline{o}_j)}} \tag{12}$$

IV. EXPERIMENTS

A. Environment for Experiments

The robot used for experiments is a wheel type self-contained mobile robot, KOMA which was developed by the authors' group(Photo.1). KOMA has rotary encoders to detect wheel rotation angular velocity. Both wheels are driven by DC motors of 20W. One PB9-01 and ultrasonic sensor array to recognize the environment are attached on the front of the body. The controller of KOMA composes of two parts: the main controller for navigation, motion control and positioning and the auxiliary controller for supporting the main controller in complex calculation of amount of data.

The map was constructed in off-line mode using previously obtained data while the robot was moving with the remote controller, in real world. In the initial map, each cell has probability value of 0.5, and initial position of the robot is set to $(x_{pos}, y_{pos}) = (330.0, -330.0)$. Tables II illustrate the parameters used for the map building experiments.

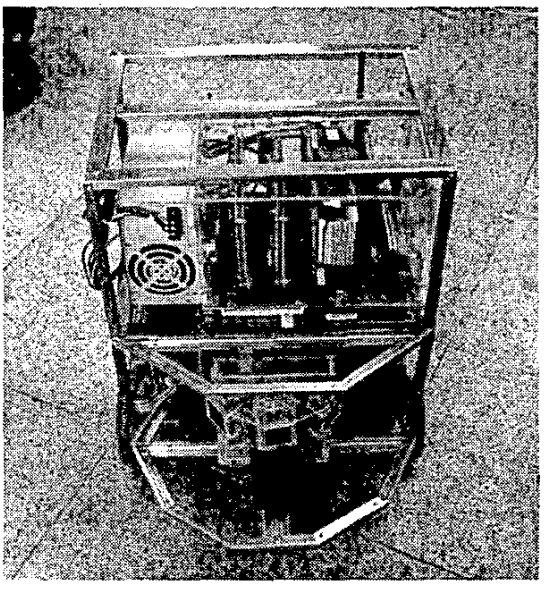

Photo. 1 Mobile robot KOMA

TABLE II
Parameters for experiments

Items	Parameters
Cell size	5×5cm
Global map size	1750×1750 cm
Cell numbers of global map	351×351 EA
Local map size	600×600cm
Cell numbers of local map	121×121 EA

Fig. 9 shows an experimental environment for verification. A hexahedral type of obstacle and a glossed cabinet were located at point A and B, respectively, and several obstacles were located at point C, irregularly. The aim of KOMA starts at C, moves to the lecture room, and finally returns to C. In this experiment, the average speed of robot was about 18.367cm/sec and total number of sensing for map building was 635.

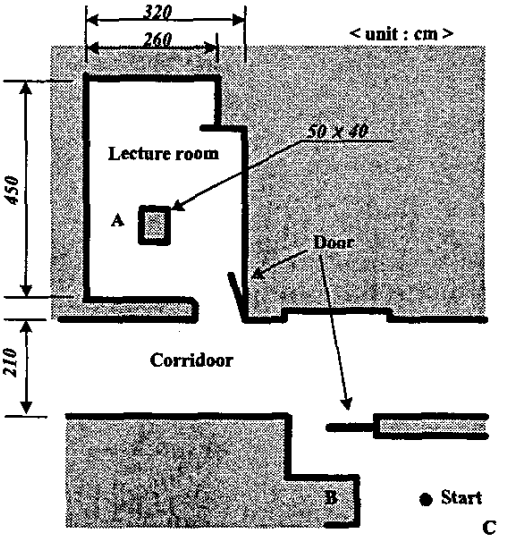

Fig. 9 Experimental environment for real world mapping

B. Experimental Results

Fig. 10 shows the result of the direct mapping using only the output of the NN corrector without probabilistic processing of sensor readings. As the result, the influence due to the random error of sensor reading is not removed.

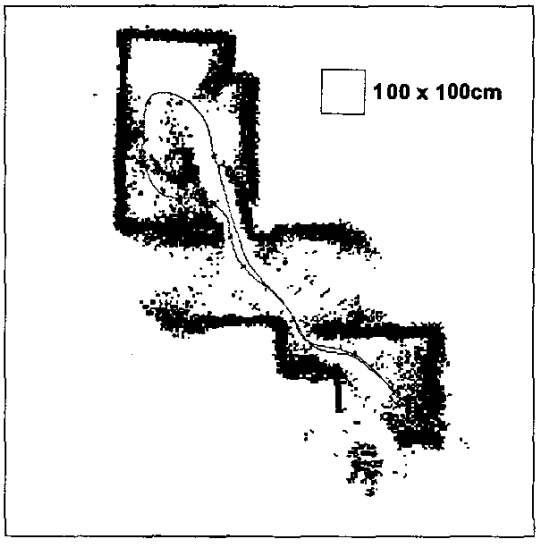

Fig. 10 Result of real world mapping before probabilistic processing

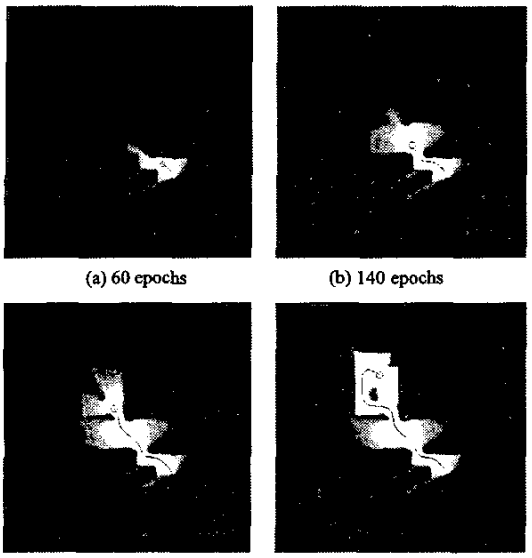

(a) 60 epochs (b) 140 epochs

(c) 240 epochs (d) 450 epochs

Fig. 11 Process of the real world mapping

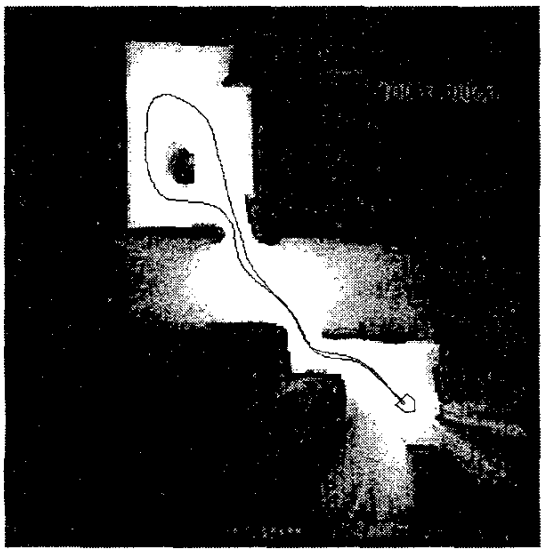

Fig. 12 Result of real world mapping after probabilistic processing

Fig. 11 shows a process of map building using the proposed algorithm for environment given in Fig. 9. In these figures, polygon indicates the robot and solid line indicates its movement trajectory. The final result of the environmental map building is shown in Fig. 12. It was found through experiments that the map is certainty similar in shape to real experimental environment from this result and the proposed map building algorithm is robust to the sensor fault due to specular reflection at the region of B.

V. CONCULSION

This work has considered the problem of building a highly accurate environmental map for a mobile robot using low-cost infrared range-finder sensors. In this work, the nonlinearity error of infrared range-finder sensors and the random error of readings are corrected by neural networks and a probabilistic approach. The proposed algorithm was implemented and tested on the experimental robot. Through experiments, we concluded:

(1) The readings error due to nonlinearity is greatly reduced by the correction using neural network.

(2) It is possible to build a high accuracy environmental map using low-cost infrared range finder sensors, through the proposed algorithm based on the probabilistic sensor model.

(3) The proposed algorithm is robust to the sensor fault caused by specular reflection.

VI. REFRENCES

[1] M. Abidi and R. Gonzalez, *Data Fusion in Robotics and Machine Intelligence,* Academic Press. Inc, 1992

[2] H. Moravec and D. W. Cho, "A Bayesian Method for Certainty Grids", *Working Notes of AAAI 1989 Spring Symposium on Robot Navigation*, pp.57-60, 1989

[3] T. Yata and A. Ohya, "A Fast and Accurate Sonar- ring Sensor for a Mobile Robot", *Proc. IEEE Int. Conf. on Robotics and Automation*, 1999

[4] A. Papoulis, *Probability , Random Variables and Stochastic Processes*, McGraw-Hill Book Co., N.Y., 1984

[5] H. Moravec, "Sensor Fusion in Certainty Grids for Mobile Robots", *AI Magazine*, Vol.9, No.2, pp.61-74, 1988

[6] M. C. Martin and H. Moravec, *Robot Evidence Grids*, Tech. Report CMU-RI-TR-96-06, Robotics Institute, Carnegie Mellon University, 1996